Oxygen isotopes in detrital zircons: Insight into crustal recycling during the evolution of the Greenland Shield

C.L. Kirkland[1,3*†], M.J. Whitehouse[1], V. Pease[2], and M. Van Kranendonk[3,4]

[1]SWEDISH MUSEUM OF NATURAL HISTORY, BOX 50007, SE-104 05 STOCKHOLM, SWEDEN
[2]DEPARTMENT OF GEOLOGY & GEOCHEMISTRY, STOCKHOLM UNIVERSITY, SE-106 91 STOCKHOLM, SWEDEN
[3]GEOLOGICAL SURVEY OF WESTERN AUSTRALIA, DEPARTMENT OF MINES AND PETROLEUM, 100 PLAIN STREET, EAST PERTH, WA 6004, AUSTRALIA
[4]SCHOOL OF EARTH AND GEOGRAPHICAL SCIENCES, UNIVERSITY OF WESTERN AUSTRALIA, 35 STIRLING HWY., CRAWLEY WA 6009, AUSTRALIA

ABSTRACT

Insight into the interactions between crust and hydrosphere, through the protracted evolution of the Greenland Shield, can be provided by oxygen isotopes in the mineral remnants of its denuded crust. Detrital zircons with ages of 3900 Ma to 900 Ma found within an arkosic sandstone dike of the Neoproterozoic (?Marinoan) Mørænesø Formation, North Greenland, provide a time-integrated record of the evolution of part of the Greenland Shield. These zircon grains are derived from a wide variety of sources in northeastern Laurentia, including Paleoproterozoic and older detritus from the Committee-Melville orogen, the Ellesmere-Inglefield mobile belt, and the subice continuation of the Victoria Fjord complex. Archean zircon crystals have a more restricted range of $\delta^{18}O_{SMOW}$ values (between 7.2‰ and 9.0‰ relative to standard mean ocean water [SMOW]) in comparison to Paleoproterozoic 1800–2100 Ma grains, which display significant variation in $\delta^{18}O_{SMOW}$ (6.8‰–10.4‰). These data reflect differences in crustal evolution between the Archean and Proterozoic Earth. Through time, remelting or reworking of high $\delta^{18}O$ materials has become more important, consistent with the progressive emergence of buoyant, cratonized continental lithosphere. A secular increase in the rate of crustal recycling is implied across the Archean-Proterozoic boundary. This rate change may have been a response to differences in the composition of sediments and/or the stabilization of continental crust.

One Eoarchean oscillatory-zoned zircon grain, free of cracks and with concordant U-Pb systematics, has an elevated $\delta^{18}O_{SMOW}$ value of 7.8‰. This is interpreted to reflect a primary magmatic signature, supporting the presence of heavy oxygen that may be compatible with a hydrosphere on early Earth, as previously determined only from Jack Hills zircons.

LITHOSPHERE; v. 2; no. 1; p. 3–12. doi: 10.1130/L80.1

INTRODUCTION

The Greenland Shield can be divided into three basement provinces, namely: (A) Archean rocks (3100–2600 Ma, with local older units up to ca. 3900 Ma) that have been essentially unaffected by Proterozoic or later orogenic activity; (B) Archean terranes that were reworked in the early Proterozoic ca. 1850 Ma; and (C) terranes composed of juvenile early Proterozoic crust (2000–1750 Ma old; Henriksen et al., 2000). Direct study is limited to exposures around the edge of the Greenland Ice Sheet. However, a complementary record of the crustal evolution of these basement blocks is available from detrital (sedimentary rock–hosted) zircon crystals that are derived from them. Zircon is a refractory mineral and is a common accessory phase in intermediate to acid igneous rocks, high-grade metamorphic rocks, and clastic sedimentary rocks. Zircon grains can survive multiple episodes of magmatic and metamorphic reworking as well as transport via the sedimentary rock cycle. Detrital zircon grains carry with them important information on crustal evolution, and a multigrain population may elucidate the evolution of vast tracts of crust (e.g., Fedo et al., 2003). Thus, they have potential to preserve a more complete record of igneous episodes than the fragmentary exposed basement of a region (e.g., Knudsen et al., 1997).

Analysis of oxygen isotopes in detrital igneous zircon crystals of known age can be used to trace both the evolution of crustal recycling and crust-mantle interaction (e.g., Valley et al., 2005). Zircon crystals diffuse oxygen slowly, even under high-temperature conditions, and hence their measured $\delta^{18}O$ value can approximate the crystallization value, provided that no late alteration has occurred (Peck et al., 2001). Incorporation of high $\delta^{18}O$ material, for example, rocks and/or minerals altered by low-temperature near-surface processes, will increase the $\delta^{18}O$ value of a melt. Hence, the zircon crystallized from such melts will also have elevated $\delta^{18}O$ values. For example, granites with a dominant metasedimentary component have bulk-rock $\delta^{18}O_{SMOW}$ values of 9‰–15‰ relative to standard mean ocean water (SMOW) (O'Neil and Chappell, 1977) and would crystallize zircon in the range ~7‰–13‰ (e.g., Lackey et al., 2005), whereas zircons in equilibrium with mantle-derived melts have $\delta^{18}O_{SMOW}$ values of ~5.3‰ ± 0.6‰ (two standard deviations; Valley, 2003). Changes in whole-rock $\delta^{18}O$ values do occur during temperature decreases accompanying magmatic differentiation (Valley, 2003), but these effects are small over the typical range of magmatic zircon crystallization temperature. Therefore, significant deviations of $\delta^{18}O$ in zircon from mantle values are primarily the consequence of magma interaction with materials altered by low-temperature near-surface processes. A $\delta^{18}O$ value of ~6.3‰–6.5‰ is commonly taken as the value above which incorporation of an elevated $\delta^{18}O$ component is implied (Valley, 2003; Cavosie et al., 2005; Kemp et al., 2006). It is noteworthy that zircon grains crystallized in both young ocean crust (e.g., Cavosie et al., 2009) and lunar melts (e.g., Nemchin et al., 2006b) have $\delta^{18}O_{SMOW}$ values less than this limit.

A compilation of $\delta^{18}O$ values in igneous zircons of known age has been used to trace the

*Corresponding author e-mail: Chris.Kirkland@dmp.wa.gov.au.
†Current address: Geological Survey of Western Australia.

evolution of intracrustal recycling and crust-mantle interaction through Earth history (Valley et al., 2005). This data set raises two significant questions: (1) Does it truly reflect global processes, given that early Earth tectonic styles may have varied in space and time, as they do on modern Earth, with crust formed through plumes and through subduction and/or accretion at the same time in different places (e.g., Foulger et al., 2005)? (2) Was the Archean homogeneous in terms of crustal recycling from 4400 to 2500 Ma (as indicated by Valley et al., 2005, their Fig. 4), which is in apparent contrast to many models for Earth evolution and crustal growth over this period (e.g., Collerson and Kamber, 1999)?

In order to help address these questions, we analyzed oxygen isotopes in detrital zircons from a sedimentary sample of the Neoproterozoic (?Marinoan) Mørænesø Formation (CKG38) from North Greenland (Fig. 1). Results from this study contribute data from previously unsampled orogens to the terrestrial oxygen isotope data set. This permits a more thorough evaluation of crustal maturation on a global scale, and it allows us to test the global applicability of the $\delta^{18}O$ evolution model (Valley et al., 2005).

Significantly, the data illustrate a more gradual secular change in magmatic $\delta^{18}O$ than has been hitherto recognized. This is used to suggest an ongoing increase in the remelting or reworking of high $\delta^{18}O$ supracrustal materials through Earth history, consistent with a secular increase in the volume of continental crust (e.g., McCulloch and Bennett, 1994; Collerson and Kamber, 1999). Additionally, a single analysis from the data set confirms heavy oxygen in Eoarchean igneous rocks, previously only reported from the Yilgarn craton of Western Australia (Peck et al., 2001).

REGIONAL GEOLOGY

The Proterozoic Mørænesø Formation is preserved in a series of paleovalleys and records a range of glacial and postglacial sedimentary processes (Collinson et al., 1989). The formation lies unconformably on the Mesoproterozoic Inuiteq Sø Formation and is overlain by the Portfjeld Formation, which, at least in part, may extend back into the late Neoproterozoic (Dewing et al., 2004). The Mørænesø Formation is thus broadly constrained in age between ca. 1380 Ma, the age of dolerites that cut the Inuiteq Sø Formation, but not the Mørænesø Formation (Upton et al., 2005), and the late Neoproterozoic (ca. 590–580 Ma). The stratigraphy of the deposit, which consists of carbonates directly overlying diamictites, has prompted correlations with Neoproterozoic Marinoan-Varanger glaciations (Surlyk, 1991).

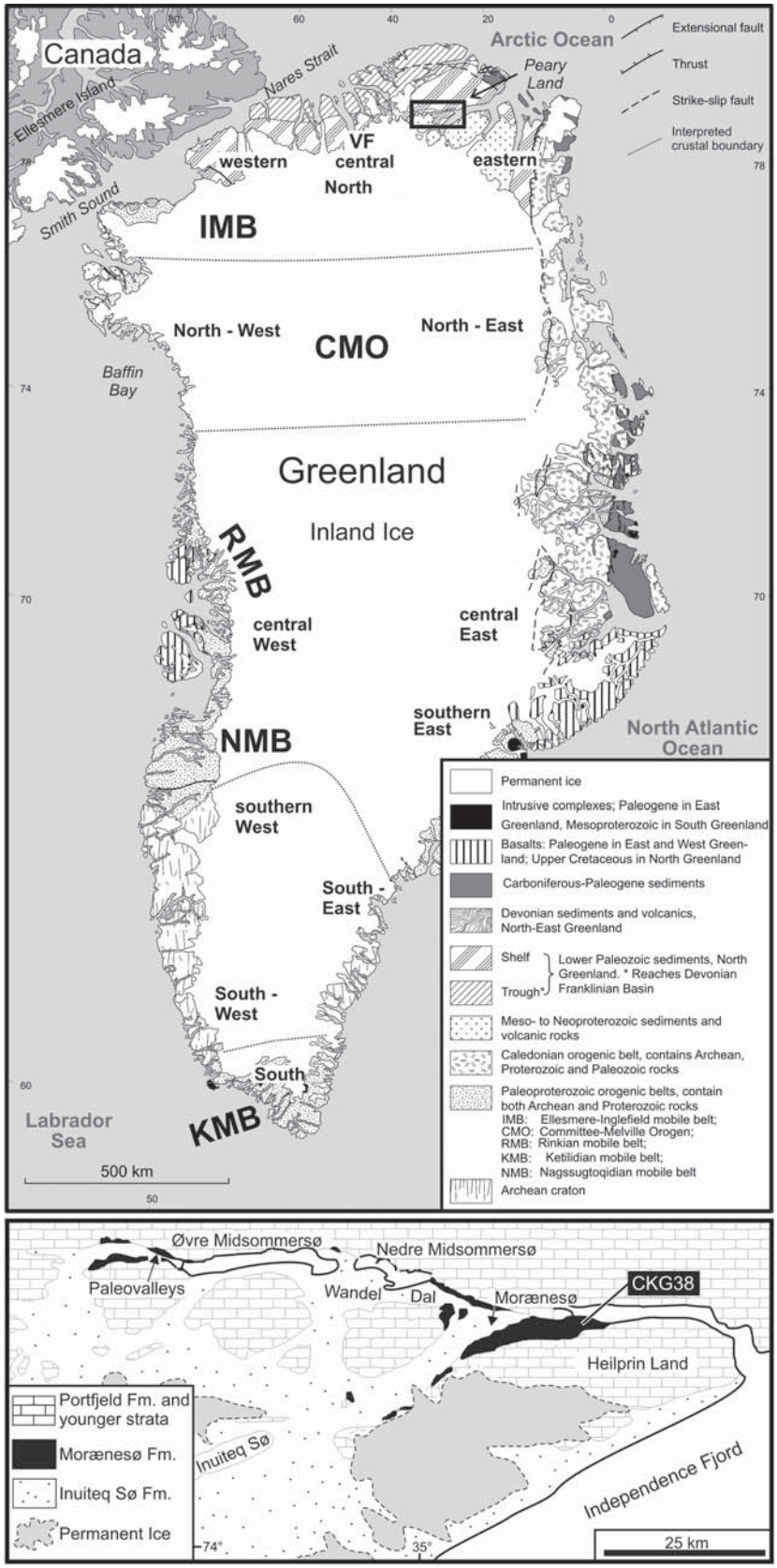

Figure 1. Geological map of Greenland based on Escher and Pulvertaft (1995). The study area in Peary Land is enclosed in a box. VF—Victoria Fjord. Inset shows enlargement of the local geology within the study area.

The sample from the Mørænesø Formation selected for this study (CKG38) represents a sandstone dike that cuts down into diamictites and is interpreted to represent a Neoproterozoic frost polygon crack filled by sand. Its zircon age distribution is typical of the Mørænesø Formation as a whole, consisting of a characteristic Mesoproterozoic to Neoproterozoic detrital zircon population, as well as prominent Paleoproterozoic (ca. 1.9–2.1 Ga) and Neoarchean populations, together with relatively minor Eoarchean-Mesoarchean components (Kirkland et al., 2009). The Mørænesø Formation is an ideal target for a regional oxygen isotope study because its detrital zircon provenance (Kirkland et al., 2009) records a wide variety of sources within northeast Laurentia, including Paleoproterozoic and older detritus from the Committee-Melville orogen, the Ellesmere-Inglefield mobile belt, and the subice continuation of the Victoria Fjord complex (e.g., Dawes, 2006; Nutman et al., 2008).

Throughout the Mørænesø Formation, the Mesoproterozoic 1000–1100 Ma Grenville detrital population appears together with ca. 1600 Ma Labradorian detritus, and thus it has been inferred that one provenance component was derived from the Grenville orogen far to the south (Kirkland et al., 2009). Rainbird et al. (1992) also reported similar detrital populations in the Minto Inlier within the Canadian high Arctic and also inferred detrital transport northward, away from the denuding Grenville orogen. The expansive source region represented by the Mørænesø Formation reflects the ability of the Marinoan fluvioglacial environment to transport material over considerable distances (Allen and Leather, 2006). In addition, it is possible that the Mørænesø Formation contains some aeolian material.

METHODS

Oxygen isotope data were obtained during three separate analytical sessions; during each session, analyses were performed in an automated sequence using a Cameca IMS1270 ion microprobe. After U-Th-Pb data acquisition and prior to oxygen isotope analysis, the zircon grains were lightly polished. As an additional precaution against bias from implanted primary beam oxygen ions, analytical locations clearly within the same crystal domain (as identified in cathodoluminescence [CL] images) but not overlapping the geochronology pit were used. The basic instrument setup and analytical procedure closely followed those described by Nemchin et al. (2006b). A 20 keV Cs+ primary beam (+10 kV primary, −10 kV secondary) of ~7 nA was used in aperture illumination mode to sputter an ~15 µm sample area. Charge compensation was provided by a normal incidence electron gun. Analytical data were acquired under fully automated runs that consisted of an ~2 min presputter with a raster of 25 µm, followed by field aperture, entrance slit and mass centering, using the ^{16}O signal. After centering, 4 min of signal integration in two Faraday detectors, operating at a common mass resolution of ~2500, measured the ^{16}O and ^{18}O isotopes. A minor linear drift correction (<1 ppm/run) was applied to the data, where applicable, in order to minimize the external error on the standards. Data were normalized to the 91500 zircon standard assuming a $\delta^{18}O_{SMOW}$ value of +9.86‰ (Wiedenbeck et al., 2004). Results obtained in three separate analytical sessions are presented in Figure 2 and Table 1 in sequential order of analysis. Overall uncertainties on $\delta^{18}O$ values are reported at the 1σ level and include a propagated external reproducibility from the standard measurements in each session that ranged from 0.21‰ to 0.24‰ (std. dev.).

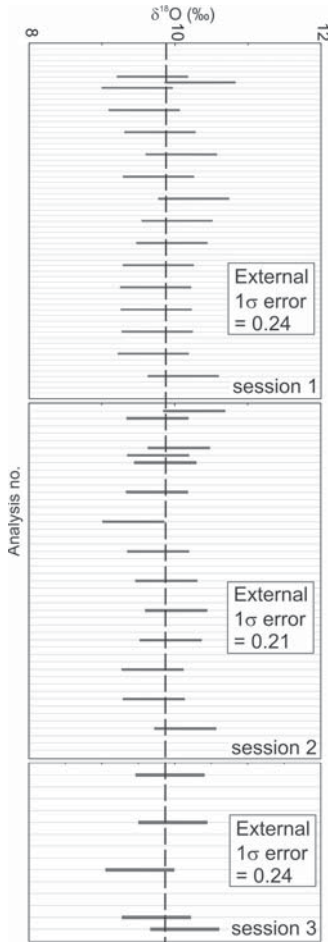

Figure 2. Sequential analyses of standard zircon 91500 during three analytical sessions (error bars are 2σ). Thin gray horizontal lines represent analyses of detrital zircon crystals.

All analytical spots were located within 6 mm of the standard and were positioned in a standard east-to-west orientation to avoid a small systematic bias observed previously in samples oriented north-south (Whitehouse and Nemchin, 2009). In all analytical sessions, there was a <50 digital units difference in DT1 centering between the sample and standard in the *y* direction and <100 units difference in the *x* direction, indicating relative flatness of the sample mount over the analyzed area.

Imaging of grains using cathodoluminescence, backscattered (BSE) and secondary electrons (SE), and reflected light optical microscopy both before and after analysis was conducted to assess data quality and significance. In particular, Cavosie et al. (2005) demonstrated that abnormal pit shape was a proxy for analyses that sampled either various amounts of fractured zircon, metamict zircon, or mounting epoxy. Using this criterion, analytical locations that could be from mixed domains, nonmagmatic zircon, inclusions, or on fractures, accounting for approximately one third of analyses, were excluded. The remaining oxygen isotope analyses from CKG38 zircons represent crystal domains (15–20 µm) that exhibit well-preserved magmatic zonation (Fig. 3) and have yielded concordant U-Pb ages (Kirkland et al., 2009); they are therefore inferred to represent magmatic values.

RESULTS

The oxygen isotope results obtained from sample CKG38 can be considered in three age sets corresponding to periods of supercontinent assembly (Condie, 1998, 2004): ca. 1000–1400 Ma Rodinia; ca. 1800–2100 Ma Paleoproterozoic; and ca. 2500–3000 Ma Archean (Table 2; Fig. 4). The Archean zircons display a relatively restricted range of $\delta^{18}O$ values of between 7.2‰ and 9.0‰ (average 8.1‰ ± 1.0‰, 2 std. dev.), in comparison to Paleoproterozoic grains that display variation in $\delta^{18}O$ from 6.8‰ to 10.4‰, with an average of ~8.0‰ ± 2.2‰ (2 std. dev.) for crystals interpreted to retain magmatic values (Fig. 4). Rodinian-aged grains (1000–1400 Ma) span a considerable range of $\delta^{18}O$ values, from ~6.5‰ to 11.9‰ (Fig. 2), within the range reported by Peck et al. (2000) from the Grenville Province. Two late Grenvillian (ca. 1050 Ma) crystals have $\delta^{18}O$ values greater than 10‰, and one ca. 1180 Ma grain has a value of 11.5‰.

DISCUSSION

The Paleoproterozoic and Archean detrital zircon populations studied herein most probably

originated from the North-West and western North Greenland regions (Kirkland et al., 2009), which include the Committee-Melville orogen (Archean), the Ellesmere-Inglefield mobile belt (Paleoproterozoic), and the subice continuation of the Victoria Fjord complex (Archean) (Dawes, 2006; Nutman et al., 2008). The crystalline rocks in this region of Greenland record an apparently continuous increase in oxygen isotopic values from a relatively restricted range in the Archean, with values less than ~9‰, to more variable $\delta^{18}O$ values in the Proterozoic, including much higher values of ~12‰. As shown in Figure 4, there appears to be a change in the rate at which oxygen isotopic values increased with time across the Archean-Proterozoic boundary, broadly consistent with—but in detail different from—the findings of Valley et al. (2005).

Archean Zircons

Significant numbers of Archean zircons in CKG38 have $\delta^{18}O$ values greater than 7.5‰, which has previously been proposed as the upper limit for Archean zircon grains (Cavosie et al., 2005; Valley et al., 2002, 2005). Fifteen Archean (>2500 Ma) grains analyzed have concordant U-Pb systematics with igneous-like Th-U ratios and low common Pb contents. These grains have either sharp oscillatory zoning or domains of oscillatory zoning overgrown by rims with homogeneous, low-cathodoluminescence response. Oscillatory-growth zoning is interpreted as a primary magmatic feature. The oldest identified, oscillatory-zoned, magmatic grain has a concordia age of 3953 ± 18 Ma (2σ), and is one of a few reported detrital Eoarchean magmatic zircons from Greenland (Fig. 3). The oxygen isotope analytical spot was sited away from any visible fractures and has a calculated accumulated alpha-radiation dosage of 0.254×10^{16} events/mg, based on age, U and Th concentrations, a value that correlates with a "well-crystallized" structure (Murakami et al., 1991). Its oxygen isotopic composition of 7.76‰ ± 0.50‰ (2σ) is greater than that observed in crystals in high-temperature equilibrium with mantle rocks (i.e., 5.3‰ ± 0.6‰; Valley, 2003). All other Archean grains analyzed herein also show elevated oxygen signatures in excess of mantle-like values. Excluding the possibility of unrecognized low-temperature disturbance, which we have attempted to identify within these concordant analyses, the elevated values thus indicate the presence of heavy oxygen by at least the Eoarchean, consistent with evidence for recycling of sedimentary rocks in early Earth history (Chauvel et al., 2008; Shirey et al., 2008).

TABLE 1. OXYGEN ISOTOPE ANALYSIS OF CKG38

Spot I.D.	Sequential number*	Standard	Background corrected $^{18}O/^{16}O$†			$\delta^{18}O$§ (‰)		
Session 1								
91500-1.1	1	std	0.00202447	±	17	9.68	±	0.26
n2539-1	2		0.00202116	±	13	8.03	±	0.25
n2539-2	3		0.00202054	±	16	7.72	±	0.26
n2539-3	4		0.00202072	±	14	7.81	±	0.25
91500-1.2	5	std	0.00202581	±	10	10.35	±	0.25
n2539-5	6		0.00202092	±	18	7.91	±	0.26
n2539-6	7		0.00202267	±	18	8.78	±	0.26
91500-1.3	8	std	0.00202405	±	14	9.47	±	0.25
n2539-7	9		0.00202291	±	23	8.90	±	0.27
n2539-8	10		0.00202756	±	17	11.22	±	0.26
n2539-9	11		0.00202523	±	20	10.06	±	0.26
91500-1.4	12	std	0.00202425	±	12	9.57	±	0.25
n2539-11	13		0.00202239	±	23	8.65	±	0.27
n2539-12	14		0.00202034	±	16	7.62	±	0.25
n2539-13	15		0.00202533	±	12	10.11	±	0.25
91500-1.5	16	std	0.00202469	±	11	9.79	±	0.25
n2539-15	17		0.00202182	±	18	8.36	±	0.26
n2539-16	18		0.00201936	±	18	7.13	±	0.26
n2539-17	19		0.00203048	±	25	12.68	±	0.27
91500-1.6	20	std	0.00202528	±	19	10.09	±	0.26
n2539-18	21		0.00202820	±	20	11.54	±	0.26
n2539-19	22		0.00202654	±	13	10.71	±	0.25
n2539-20	23		0.00202050	±	21	7.70	±	0.26
91500-1.7	24	std	0.00202465	±	23	9.77	±	0.27
n2539-21	25		0.00201983	±	21	7.37	±	0.26
n2539-23	26		0.00201995	±	12	7.43	±	0.25
n2539-24	27		0.00202305	±	24	8.98	±	0.27
91500-1.8	28	std	0.00202562	±	17	10.26	±	0.26
n2539-25	29		0.00202328	±	14	9.09	±	0.25
n2539-26	30		0.00201949	±	15	7.20	±	0.25
n2539-29	31		0.00202161	±	15	8.25	±	0.25
91500-1.9	32	std	0.00202517	±	15	10.03	±	0.25
n2539-31	33		0.00202440	±	17	9.65	±	0.26
n2539-33	34		0.00202193	±	19	8.41	±	0.26
n2539-34	35		0.00202453	±	15	9.71	±	0.25
91500-1.10	36	std	0.00202502	±	17	9.95	±	0.26
n2539-35	37		0.00201798	±	22	6.45	±	0.27
n2539-36	38		0.00202046	±	11	7.68	±	0.25
n2539-37	39		0.00202246	±	21	8.68	±	0.26
91500-1.11	40	std	0.00202463	±	17	9.76	±	0.26
n2539-38	41		0.00202029	±	22	7.60	±	0.27
n2539-39	42		0.00202055	±	14	7.73	±	0.25
n2539-41	43		0.00202023	±	15	7.57	±	0.25
91500-1.12	44	std	0.00202457	±	15	9.73	±	0.25
n2539-42	45		0.00202733	±	22	11.11	±	0.27
n2539-43	46		0.00202103	±	14	7.96	±	0.25
n2539-44	47		0.00201505	±	31	4.98	±	0.29
91500-1.13	48	std	0.00202459	±	12	9.74	±	0.25
n2539-46	49		0.00201741	±	15	6.16	±	0.25
n2539-47	50		0.00202220	±	23	8.55	±	0.27
n2539-48	51		0.00202065	±	18	7.78	±	0.26
91500-1.14	52	std	0.00202461	±	11	9.75	±	0.25
n2539-49	53		0.00202353	±	21	9.21	±	0.26
n2539-51	54		0.00202380	±	16	9.35	±	0.26
n2539-b19	55		0.00202062	±	16	7.76	±	0.25
91500-1.14	56	std	0.00202450	±	13	9.70	±	0.25
n2539-b18	57		0.00201977	±	21	7.34	±	0.26
n2539-b20	58		0.00201951	±	17	7.21	±	0.26
n2539-b21	59		0.00201866	±	17	6.78	±	0.26
91500-1.15	60	std	0.00202533	±	18	10.11	±	0.26
n2539-b22	61		0.00202521	±	24	10.05	±	0.27
n2539-b25	62		0.00202771	±	19	11.30	±	0.26
n2539-b27	63		0.00201943	±	22	7.17	±	0.27

(*continued*)

TABLE 1. OXYGEN ISOTOPE ANALYSIS OF CKG38 (*continued*)

Spot I.D.	Sequential number*	Standard	Background corrected $^{18}O/^{16}O$†			$\delta^{18}O$§ (‰)		
Session 2								
91500-2.1	1	std	0.00202768	±	18	10.27	±	0.23
91500-2.2	2	std	0.00202666	±	14	9.76	±	0.22
n2539-b27_31	3		0.00202794	±	15	10.40	±	0.22
n2539-b29	4		0.00202485	±	21	8.86	±	0.24
n2539-b3	5		0.00202298	±	15	7.93	±	0.22
91500-2.3	6	std	0.00202725	±	14	10.05	±	0.22
91500-2.3	7	std	0.00202668	±	17	9.77	±	0.23
91500-2.4	8	std	0.00202688	±	13	9.87	±	0.22
n2539-b30	9		0.00202391	±	16	8.39	±	0.23
n2539-b34	10		0.00202115	±	13	7.01	±	0.22
n2539-b35	11		0.00202728	±	21	10.07	±	0.24
91500-2.5	12	std	0.00202665	±	14	9.75	±	0.22
n2539-b37	13		0.00202325	±	24	8.06	±	0.24
n2539-b4	14		0.00202388	±	30	8.38	±	0.26
n2539-b40	15		0.00202463	±	24	8.75	±	0.24
91500-2.6	16	std	0.00202599	±	17	9.43	±	0.23
n2539-b41	17		0.00202392	±	23	8.39	±	0.24
n2539-b43	18		0.00202676	±	23	9.81	±	0.24
n2539-b44	19		0.00203209	±	21	12.46	±	0.24
91500-2.7	20	std	0.00202668	±	18	9.77	±	0.23
n2539-b45	21		0.00202554	±	21	9.20	±	0.24
n2539-b47	22		0.00202318	±	14	8.02	±	0.22
n2539-b48	23		0.00202450	±	22	8.68	±	0.24
91500-2.8	24	std	0.00202690	±	15	9.88	±	0.22
n2539-b49	25		0.00202776	±	22	10.31	±	0.24
n2539-b5	26		0.00202652	±	19	9.69	±	0.23
n2539-b55	27		0.00202297	±	31	7.92	±	0.26
91500-2.9	28	std	0.00202718	±	17	10.02	±	0.23
n2539-b56	29		0.00202313	±	12	8.00	±	0.22
n2539-b57	30		0.00202595	±	23	9.40	±	0.24
n2539-b58	31		0.00202241	±	26	7.64	±	0.25
91500-2.10	32	std	0.00202703	±	16	9.94	±	0.23
n2539-b59	33		0.00202237	±	19	7.62	±	0.23
n2539-b6	34		0.00202270	±	15	7.79	±	0.22
n2539-b60	35		0.00202461	±	16	8.74	±	0.23
91500-2.11	36	std	0.00202652	±	16	9.69	±	0.23
n2539-b61	37		0.00202476	±	27	8.81	±	0.25
n2539-b63	38		0.00202694	±	23	9.90	±	0.24
n2539-b65	39		0.00203529	±	10	14.06	±	0.22
91500-2.12	40	std	0.00202656	±	17	9.71	±	0.23
n2539-b68	41		0.00202566	±	24	9.26	±	0.24
n2539-b69	42		0.00202366	±	27	8.26	±	0.25
n2539-b70	43		0.00202260	±	18	7.74	±	0.23
91500-2.13	44	std	0.00202743	±	21	10.14	±	0.24
n2539-b71	45		0.00202593	±	17	9.40	±	0.23
n2539-64	46		0.00202151	±	21	7.20	±	0.24
n2539-65	47		0.00202103	±	23	6.95	±	0.24
Session 3								
91500-3.1	1	std	0.00202075	±	21	9.93	±	0.26
n2539-a60	2		0.00202060	±	24	9.86	±	0.27
n2539-a61	3		0.00201959	±	18	9.35	±	0.25
n2539-a62	4		0.00202491	±	25	12.01	±	0.27
91500-3.2	5	std	0.00202083	±	14	9.97	±	0.25
n2539-b10	6		0.00202144	±	18	10.28	±	0.25
n2539-b12	7		0.00201795	±	25	8.53	±	0.27
n2539-b14	8		0.00202546	±	25	12.29	±	0.27
91500-3.3	9	std	0.00201990	±	16	9.51	±	0.25
n2539-b16	10		0.00202328	±	22	11.20	±	0.26
n2539-b17	11		0.00201823	±	26	8.68	±	0.27
n2539-b2	12		0.00202521	±	27	12.16	±	0.27
91500-3.4	13	std	0.00202037	±	12	9.74	±	0.24
91500-3.5	14	std	0.00202116	±	10	10.14	±	0.24

Note: Each $\delta^{18}O$ error (1σ) represents the sum of counting statistics errors for each individual spot and the external error based on all standards analyzed during the session, which were added in quadrature.
*In sequential order of analyses.
†Raw ratios corrected for measured Faraday offsets and yields; absolute error is presented ×10^8.
§Normalized to a $\delta^{18}O$ value of 9.86‰ for the 91500 standard.

Similar results from other Eoarchean to Hadean zircon crystals in the Jack Hills of Western Australia have led to marked differences in interpretation (e.g., Coogan and Hinton, 2006; Harrison et al., 2005; Nemchin et al., 2006a). Oxygen isotope and trace-element zonation from Jack Hills zircon has been suggested as evidence for Hadean igneous processes involving supracrustal material (Wilde et al., 2001). Unradiogenic Hf isotope compositions in other ancient Jack Hills zircons imply the existence of enriched (crustal) reservoirs by at least 4300 Ma (Amelin et al., 1999; Harrison et al., 2005). However, both the size of this crust and the mechanism whereby it was generated are debated (e.g., Shirey et al., 2008). Thermobarometry of mineral inclusions within Jack Hills zircons indicates that they formed in a region with low heat flow, consistent with, but not exclusive to, a subduction-zone setting (Hopkins et al., 2008; Rollinson, 2008; Nutman et al., 2008). Detailed discussion of the significance of Hadean Jack Hills zircon has been presented elsewhere (e.g., Cavosie et al., 2005; Nemchin et al., 2006a) and is not reiterated here.

While the oxygen isotopic data from Greenland cannot, on its own, resolve the question as to when subduction initiated on early Earth, it can help to elucidate the conditions for melting in the Eoarchean Greenland Shield. Our oxygen isotope results suggest that the majority of detrital zircons in the Mørænesø Formation were derived from melts that incorporated material modified by near-surface processes. The host melts to these detrital zircon crystals appear to have been generated during crustal reworking events accompanying supercontinent assembly (Condie, 1998, 2004). Additionally, the heavy oxygen signature in a single Eoarchean zircon is consistent with the presence of liquid water at ca. 4 Ga, permitting wet melting conditions. This documents that the heavy oxygen isotopic signal from the Jack Hills zircons is not unique to the Yilgarn of Western Australia, but it is also recorded in Eoarchean grains from other cratons.

Paleoproterozoic Zircons

Several high $\delta^{18}O$ values were obtained from Paleoproterozoic grains. However, these grains have a homogeneous low-cathodoluminescence response and show no textural evidence of retaining a primary magmatic signature, such as oscillatory-growth zoning (e.g., Nemchin et al., 2006a). The oxygen isotope compositions for these grains therefore could reflect a variety of nonmagmatic alteration processes, including interaction with low-temperature surface or subsurface water, which could have resulted in elevated $\delta^{18}O$ values for these

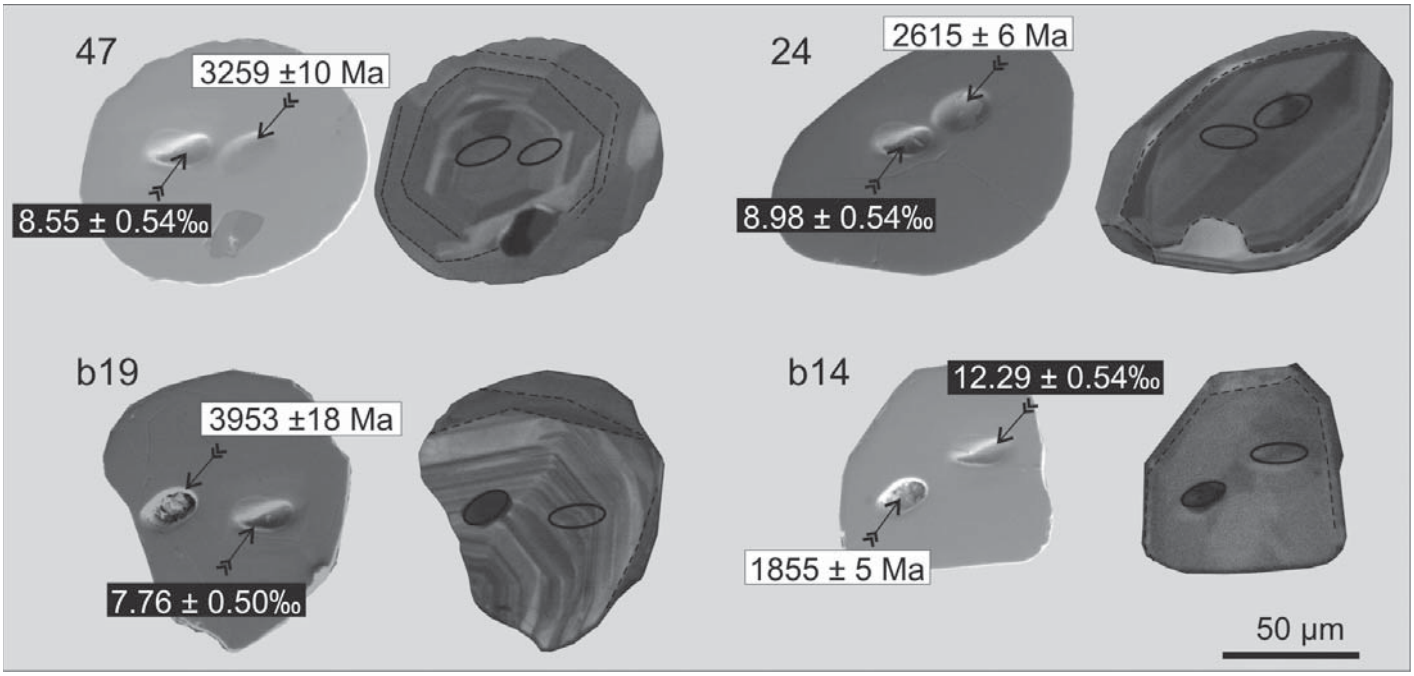

Figure 3. Cathodoluminescence (right) and secondary electron (left) images of selected detrital zircons from the Morænesø Formation (CKG38). $\delta^{18}O$ values (2σ) are shown in black filled boxes; concordia ages are given in white filled boxes. Grain b14 has no features conclusively indicating a magmatic heritage. All other grains are interpreted to preserve magmatic $\delta^{18}O$ values and have been dated within the same textural domain as oxygen isotope analysis.

TABLE 2. GEOCHRONOLOGICAL AND OXYGEN ISOTOPES IN DETRITAL ZIRCON GRAINS FROM THE MORÆNESØ FORMATION
CKG38 (82.1706963/–31.3823337)

Sample/ spot no.	[U] (ppm)	[Th] (ppm)	Th/U (meas.)	f_{206} (%)	Disc. % (conv.)	$^{207}Pb/^{206}Pb$	±σ	$^{206}Pb/^{238}U$	±σ	$\delta^{18}O$ (‰)	±σ	No. alpha events/mg (×10^{15})	Calc. density (g/cm^3)
n2539-42	280	67	0.240	0.09	5.9	971	26	1024	8	*11.11*	*0.27*	1.02	4.70
n2539-35	192	50	0.260	0.05	3.8	986	22	1020	8	**6.45**	**0.27**	0.72	4.72
n2539-a62	458	110	0.240	{0.02}	4.1	986	23	1023	11	**12.01**	**0.27**	1.70	4.64
n2539-9	210	107	0.510	0.05	6.1	993	18	1049	8	**10.06**	**0.26**	0.83	4.71
n2539-23	102	27	0.270	0.06	3.2	1067	18	1098	8	**7.43**	**0.25**	0.42	4.74
n2539-21	306	178	0.580	1.54	2.0	1071	28	1091	8	**7.37**	**0.26**	1.34	4.67
n2539-b-68	270	51	0.190	0.02	1.3	1077	7	1089	13	**9.26**	**0.24**	1.09	4.69
n2539-b-47	120	33	0.270	{0.01}	–0.2	1087	11	1086	13	*8.02*	*0.22*	0.50	4.73
n2539-18	136	47	0.350	0.05	3.0	1147	23	1179	9	**11.54**	**0.26**	0.61	4.72
n2539-b-60	123	49	0.400	{0.03}	1.6	1162	11	1179	14	*8.74*	*0.23*	0.57	4.73
n2539-b-22	209	39	0.190	0.28	–1.5	1225	19	1208	11	**10.05**	**0.27**	0.98	4.70
n2539-b-12	152	67	0.440	{0.00}	0.9	1257	10	1266	11	**8.53**	**0.27**	0.77	4.71
n2539-b-41	83	52	0.630	{0.01}	0.7	1312	12	1321	12	*8.39*	*0.24*	0.46	4.73
n2539-37	105	46	0.440	0.15	2.3	1355	28	1383	10	*8.68*	*0.26*	0.58	4.73
n2539-33	119	60	0.500	0.14	2.3	1427	21	1456	11	**8.41**	**0.26**	0.71	4.72
n2539-b-45	140	77	0.550	0.03	–0.2	1427	8	1425	13	*9.20*	*0.24*	0.84	4.71
n2539-b-30	185	111	0.600	0.04	1.5	1457	7	1477	13	**8.39**	**0.23**	1.15	4.69
n2539-16	187	77	0.410	{0.02}	–0.7	1464	16	1455	12	**7.13**	**0.26**	1.12	4.69
n2539-b-6	55	32	0.580	{0.06}	2.1	1618	14	1648	14	**7.79**	**0.22**	0.38	4.74
n2539-3	198	135	0.680	0.04	0.7	1649	11	1659	12	**7.81**	**0.25**	1.44	4.66
n2539-b-63	344	66	0.190	0.01	–0.5	1741	6	1733	19	*9.90*	*0.24*	2.43	4.57
n2539-b-61	170	92	0.540	0.02	2.7	1848	5	1890	21	*8.81*	*0.25*	1.38	4.67
n2539-44	242	270	1.120	0.03	2.4	1854	11	1893	14	*4.98*	*0.29*	2.18	4.59
n2539-b-59	132	80	0.600	{0.01}	1.6	1856	6	1881	21	**7.62**	**0.23**	1.09	4.69
n2539-b-14	218	89	0.410	{0.01}	–1.1	1857	5	1839	16	**12.29**	**0.27**	1.74	4.63
n2539-17	262	175	0.670	0.04	1.3	1867	15	1887	17	*12.68*	*0.27*	2.21	4.59
n2539-26	81	197	2.440	0.10	4.1	1877	21	1943	13	**7.20**	**0.25**	0.90	4.71
n2539-b-10	89	36	0.410	0.05	0.2	1880	12	1884	16	**10.28**	**0.25**	0.72	4.72
n2539-b-2	182	52	0.290	{0.01}	0.3	1890	6	1895	16	**12.16**	**0.27**	1.45	4.66
n2539-a61	90	50	0.550	{0.00}	1.2	1891	23	1910	24	**9.35**	**0.25**	0.75	4.72

(*continued*)

TABLE 2. GEOCHRONOLOGICAL AND OXYGEN ISOTOPES IN DETRITAL ZIRCON GRAINS FROM THE MORÆNESØ FORMATION
CKG38 (82.1706963/–31.3823337) (*continued*)

Sample/ spot no.	[U] (ppm)	[Th] (ppm)	Th/U (meas.)	f_{206} (%)	Disc. % (conv.)	$^{207}Pb/^{206}Pb$	±σ	$^{206}Pb/^{238}U$	±σ	$\delta^{18}O$ (‰)	±σ	No. alpha events/mg ($\times10^{15}$)	Calc. density (g/cm^3)
n2539-19	185	99	0.530	0.18	2.4	1891	12	1931	14	*10.71*	*0.25*	1.55	4.65
n2539-13	205	157	0.760	0.06	–0.6	1893	13	1883	14	*10.11*	*0.25*	1.79	4.63
n2539-b-16	165	87	0.530	0.04	1.4	1893	6	1916	16	**11.20**	**0.26**	1.38	4.67
n2539-b-49	220	75	0.340	{0.01}	1.2	1894	4	1913	21	**10.31**	**0.24**	1.77	4.63
n2539-b-57	261	221	0.850	0.03	0.0	1895	5	1895	22	*9.40*	*0.24*	2.31	4.58
n2539-b-44	146	54	0.370	{0.01}	–0.8	1908	6	1896	16	**12.46**	**0.24**	1.20	4.68
n2539-34	223	120	0.540	0.02	3.3	1916	13	1971	14	*9.71*	*0.25*	1.90	4.62
n2539-b-27_31	152	80	0.530	{0.00}	0.7	1917	8	1929	17	**10.40**	**0.22**	1.29	4.67
n2539-15	72	39	0.540	0.13	2.0	1919	17	1953	14	*8.36*	*0.26*	0.61	4.72
n2539-49	296	211	0.710	0.10	2.2	1921	10	1958	14	*9.21*	*0.26*	2.61	4.55
n2539-20	262	5	0.020	0.01	–1.1	1921	9	1904	13	**7.70**	**0.26**	2.02	4.61
n2539-b-35	210	113	0.540	{0.01}	1.8	1938	5	1969	17	**10.07**	**0.24**	1.81	4.63
n2539-b-71	122	111	0.910	0.02	0.8	1955	7	1968	21	*9.40*	*0.23*	1.14	4.69
n2539-b-25	215	75	0.350	0.04	–2.5	1974	8	1930	16	*11.30*	*0.26*	1.83	4.62
n2539-b-40	94	54	0.580	0.03	0.8	1974	7	1987	18	**8.75**	**0.24**	0.83	4.71
n2539-38	181	187	1.030	0.08	1.4	1978	11	2002	14	**7.60**	**0.27**	1.75	4.63
n2539-b-29	165	102	0.620	0.02	0.6	1979	6	1988	17	**8.86**	**0.24**	1.48	4.66
n2539-39	55	68	1.220	0.08	–0.6	1986	24	1976	14	**7.73**	**0.25**	0.55	4.73
n2539-b-20	66	39	0.590	0.12	0.4	1987	10	1994	17	**7.21**	**0.26**	0.60	4.73
n2539-b-5	147	69	0.470	{0.01}	–0.5	1988	7	1979	16	*9.69*	*0.23*	1.29	4.67
n2539-31	212	107	0.500	0.04	0.5	1994	9	2003	14	*9.65*	*0.26*	1.89	4.62
n2539-12	190	88	0.460	0.02	1.7	2002	11	2032	14	**7.62**	**0.25**	1.68	4.64
n2539-b-65	204	94	0.460	0.02	0.2	2006	5	2009	22	*14.06*	*0.22*	1.81	4.63
n2539-8	143	39	0.280	0.04	0.2	2015	12	2018	14	**11.22**	**0.26**	1.23	4.68
n2539-43	148	77	0.520	0.11	–0.6	2015	17	2004	16	*7.96*	*0.25*	1.34	4.67
n2539-2	151	88	0.580	0.03	0.8	2026	9	2040	14	**7.72**	**0.26**	1.38	4.67
n2539-b-43	123	101	0.820	{0.01}	–1.8	2042	7	2011	18	**9.81**	**0.24**	1.19	4.68
n2539-51	148	134	0.910	0.03	–2.0	2048	14	2013	14	**9.35**	**0.26**	1.46	4.66
n2539-b-4	117	103	0.880	0.04	–0.6	2054	7	2043	18	**8.38**	**0.26**	1.15	4.69
n2539-41	332	202	0.610	0.16	0.6	2064	9	2075	15	**7.57**	**0.25**	3.13	4.49
n2539-b-21	169	166	0.980	0.13	–0.9	2067	5	2051	17	**6.78**	**0.26**	1.71	4.64
n2539-7	83	65	0.780	0.03	2.6	2067	13	2114	17	**8.90**	**0.27**	0.81	4.71
n2539-25	97	61	0.630	0.07	1.1	2069	11	2087	15	**9.09**	**0.25**	0.92	4.70
n2539-b-34	133	85	0.640	0.03	1.7	2071	6	2101	17	**7.01**	**0.22**	1.27	4.68
n2539-b-27	52	51	0.980	{0.03}	–0.1	2142	9	2141	18	**7.17**	**0.27**	0.55	4.73
n2539-b-3	190	70	0.370	0.06	–0.7	2438	8	2424	19	*7.93*	*0.22*	2.14	4.59
n2539-b-55	205	78	0.380	{0.01}	–1.7	2492	7	2458	26	*7.92*	*0.26*	2.38	4.57
n2539-65	264	100	0.380	0.24	0.5	2513	15	2523	25	*6.95*	*0.24*	3.10	4.50
n2539-b-48	129	89	0.690	0.07	0.4	2543	5	2552	27	**8.68**	**0.24**	1.62	4.64
n2539-36	170	226	1.330	0.05	–1.5	2549	8	2518	17	**7.68**	**0.25**	2.38	4.57
n2539-48	39	47	1.190	1.67	–1.9	2587	26	2547	17	**7.78**	**0.26**	0.55	4.73
n2539-24	131	129	0.990	0.02	–0.2	2615	6	2610	18	**8.98**	**0.27**	1.79	4.63
n2539-11	287	110	0.380	0.08	2.0	2624	6	2667	18	*8.65*	*0.27*	3.58	4.45
n2539-b-37	84	47	0.560	0.04	–1.3	2672	5	2642	21	*8.06*	*0.24*	1.10	4.69
n2539-29	148	85	0.570	0.02	–1.2	2675	7	2649	18	**8.25**	**0.25**	1.96	4.61
n2539-1	228	57	0.250	0.01	2.3	2705	7	2755	20	**8.03**	**0.25**	2.91	4.52
n2539-46	108	82	0.760	0.25	–1.5	2719	10	2686	18	*6.16*	*0.25*	1.50	4.66
n2539-b-58	233	133	0.570	0.01	1.2	2720	3	2747	28	**7.64**	**0.25**	3.16	4.49
n2539-b-56	50	121	2.410	0.03	1.3	2728	6	2757	30	**8.00**	**0.22**	0.89	4.71
n2539-6	213	113	0.530	0.01	2.4	2740	10	2793	22	**8.78**	**0.26**	2.90	4.52
n2539-b-18	131	50	0.390	0.08	–0.6	2764	4	2751	22	*7.34*	*0.26*	1.76	4.63
n2539-64	170	99	0.580	{0.06}	3.3	2811	13	2886	28	**7.20**	**0.24**	2.42	4.57
n2539-b-70	38	19	0.510	0.03	–0.8	2824	12	2805	37	**7.74**	**0.23**	0.54	4.73
n2539-b-17	118	47	0.400	{0.01}	1.8	2835	6	2875	32	**8.68**	**0.27**	1.65	4.64
n2539-a60	57	52	0.900	{0.11}	1.3	3013	16	3045	29	*9.86*	*0.27*	0.95	4.70
n2539-b-69	142	54	0.380	0.02	0.4	3230	3	3241	32	*8.26*	*0.25*	2.42	4.57
n2539-47	93	124	1.330	0.03	–1.1	3266	12	3238	20	**8.55**	**0.27**	1.86	4.62
n2539-5	49	28	0.580	0.16	–1.0	3290	10	3264	20	**7.91**	**0.26**	0.89	4.71
n2539-b-19	95	59	0.620	{0.01}	–1.9	3969	21	3913	34	**7.76**	**0.25**	2.43	4.57

Note: % Disc. (conv.) is the age discordance in conventional concordia space. All errors are at the 1σ level. f_{206} is the percentage of common ^{206}Pb, estimated from the measured ^{204}Pb. Figures are given in parentheses when no correction has been applied owing to insignificant levels of ^{204}Pb. Data are arranged according to increasing $^{207}Pb/^{206}Pb$ age. Values in italic are interpreted to be unreliable due to sampling of inclusions, mixed domains, or on fractures. Oxygen isotope values in bold are interpreted to reflect primary igneous values. Oxygen isotope values in filled boxes are from homogeneous cathodoluminescence (CL) dark grains and may not represent primary values. Oxygen results in their analytical sequence, including standards, are presented in Table 1. Density and alpha dosage calculations are after Murakami et al. (1991). Numbers after the sample identification in the header refer to the position of the sample site and are in decimal degrees.

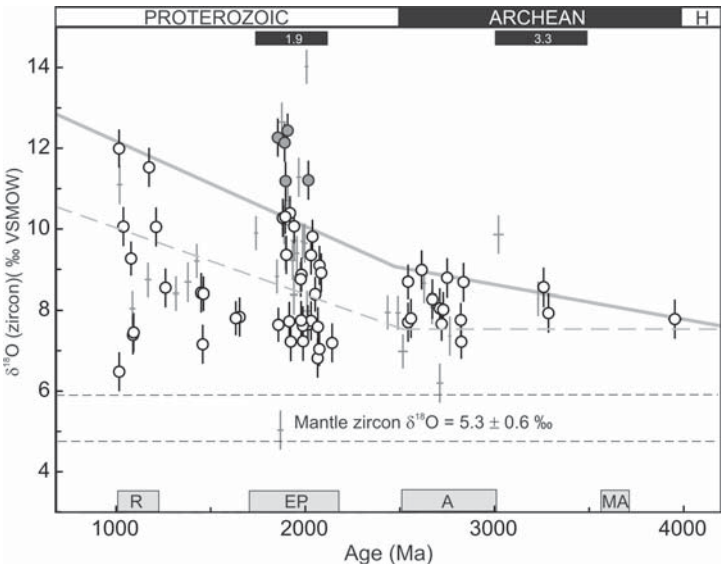

Figure 4. $\delta^{18}O$ (zircon) versus concordia age of detrital zircons from the Mørænesø Formation. Error bars are 2σ. Filled circles are from homogeneous cathodoluminescence (CL) domains and may not preserve magmatic values; gray crosses are on fractures and mixed domains; unfilled circles are interpreted to preserve primary values. Samples range in age from ca. 1000 to 4000 Ma and appear to have sampled a large region of northeast Laurentia. Archean zircons have a restricted range in $\delta^{18}O$ values of 7‰–9‰. Higher and more variable oxygen isotope values are observed in the Paleozoic, with enhanced recycling or reworking of high $\delta^{18}O$ material into magmas. The dotted line represents the highest $\delta^{18}O$ values exhibited by zircon in the compilation of Valley et al. (2005). Periods of supercontinent growth are shown by gray bars: R—Rodinia; EP—Early Proterozoic; A—Archean; MA—Middle Archean (Condie, 1998). Approximate times of juvenile crustal addition based on Hf model ages from zircons with low $\delta^{18}O$ are shown in black boxes inscribed with the age of peak addition (Kemp et al., 2006). H—Hadean.

grains. Although such alteration processes cannot be clearly identified by strong discordance, increase in common Pb, or change in Th-U ratio (e.g., Peck et al., 2003), the textural features of these grains caution that they may have experienced some minor degree of postcrystallization alteration that did not demonstrably affect their U-Pb systematics (e.g., Nemchin et al., 2006a) (Fig. 4). Therefore, we have opted for a conservative interpretation and consider these results to represent potentially modified $\delta^{18}O$ values.

Mesoproterozoic Zircons

The high $\delta^{18}O$ values (12‰) for some ca. 1000 Ma zircons obtained in this study are consistent with those of Valley et al. (2005). These grains have similar oxygen isotopic compositions to crystals in anorthosite–mangerite–charnockite–granite plutons in the Fronetenac arc of the Grenville Province, which are known to have elevated $\delta^{18}O$ values of up to 14‰ (King et al., 1998). These elevated oxygen isotopic values support the conclusion of Kirkland et al. (2009) that the detrital population of the Mørænesø Formation contains a contribution from a distal Grenville source.

Secular Change in $\delta^{18}O$

There are numerous models for both the growth of continental crust and the rate of crustal recycling through the mantle (Fyfe, 1978; Hawkesworth and Kemp, 2006; Hurley and Rand, 1969; Moorbath, 1985; Nägler and Kramers, 1998; Taylor and McLennan, 1981). The relatively uniform upper values of $\delta^{18}O$ in magmas across the whole of the Archean have been used to suggest that rates of crustal recycling balanced rates of crustal growth on early Earth (Valley et al., 2005), as also suggested for modern Earth (Scholl and von Huene, 2009). Our Greenland data, however, suggest an increase in the heaviest $\delta^{18}O$ values (albeit strongly constrained by the single Eoarchean analysis). This apparent increase in $\delta^{18}O$ may signify the increasing incorporation of high $\delta^{18}O$ materials by magmas over time. One mechanism to achieve this could be through increased weathering, transport, and subduction recycling of sedimentary material. However, there is no unique requirement for sediment subduction, since reworking in the crust leading to melting is also feasible. In either case, the change in maximum $\delta^{18}O$ value through time is consistent with a secular increase in the volume of continental crust, as suggested by a wide range of isotope and geochemical evidence (e.g., Allègre, 1982; Allègre and Rousseau, 1984; Collerson and Kamber, 1999; McLennan and Taylor, 1983; Veizer and Compston, 1976), and the decline in the rate of mantle magmatism (e.g., Dickinson and Kröner, 1981).

Changes across the Archean-Proterozoic Boundary

The Greenland data set presented shows an apparent continuous rise in $\delta^{18}O$ values throughout the Proterozoic, distinct from the Archean, and changing around the Archean-Proterozoic boundary (Fig. 3; see also Valley et al., 2005). Assuming an average sediment value of ~+15‰ and a highest Archean magmatic value of +9‰, this would imply a maximum input of ~30% high $\delta^{18}O$ material in the Archean magmas of the Greenland Shield relative to mantle $\delta^{18}O$ values. For Proterozoic zircon grains, up to ~50% of high $\delta^{18}O$ material could have been incorporated into the magmas.

These changes most likely reflect differences in the composition and/or abundance of sediment and/or altered crust available for recycling (Albarède, 1998). Other factors may account for the change in slope of the $\delta^{18}O$ values across the Archean-Proterozoic boundary, such as the development of cyanobacteria and the rise in atmospheric oxygen. In the Archean, an atmosphere exhibiting higher pCO_2 and possibly pCH_4 would result in higher degrees of chemical weathering (Kump, 2008), and dissolved weathered rocks would be transported into the oceans as solutes mixing with the bulk ocean. The resulting subduction-related magmas (produced from material derived or influenced by the oceans) would thus reflect isotopic dilution by the water mass and the buffering effects of ocean crust alteration at mid-ocean ridges (e.g., Jean-Baptiste et al., 1997). After the development of an oxygenic atmosphere, however, the style of rock weathering changed to a regime of principally physico-mechanical breakdown of materials (e.g., Condie, 1993; Lowe and Tice, 2004). Hence, oxygen isotope signatures in zircons produced from material affected by near-surface processes, where fractionation is large, remained locked within the mineral grains and were preserved for later reworking.

Another possible factor accounting for the change in slope of the $\delta^{18}O$ values across the Archean-Proterozoic boundary is the

development of larger, cooler, and stiffer plates by the end of the Archean. This would have given rise to longer, higher orogens (Campbell and Allen, 2008; Squire et al., 2006). In this model, rates of sediment recycling in the Archean were limited by a lack of uplift and erosion of continents. This limit reflects greater radiogenic heat production, as judged from K, Th, and U, in the Archean (e.g., O'Nions et al., 1978; Davies, 1980; Wanke et al., 1984; Franck, 1998), which resulted in softer, weaker continental lithosphere (Cagnard et al., 2006; Choukroune et al., 1995; Rey and Houseman, 2006). This inherent weakness meant that continental crust did not significantly thicken upward during subduction-accretion and continental collision events (e.g., the widespread development of low-grade granite-greenstone terrains), and hence there was limited uplift and erosion. In the Proterozoic, secular decrease in radioactivity and overall mantle heat, combined with melt depletion of lower crust (Rudnick and Fountain, 1995), would have resulted in larger plates and progressive strengthening of continental lithosphere, in turn allowing crustal thickening, uplift, orographic precipitation, and erosion at greater rates and volumes than in the Archean. This would have increased sediment recycling, thereby increasing the $\delta^{18}O$ values of Proterozoic magmas.

CONCLUSIONS

The $\delta^{18}O$ values of detrital zircon crystals in the Mørænesø Formation indicate a maximum input of ~30% high $\delta^{18}O$ material into Archean magmas of the Greenland Shield relative to the mantle. For Proterozoic zircons, up to ~50% of high $\delta^{18}O$ material could have been incorporated into these magmas. Therefore, recycling of high $\delta^{18}O$ sources, such as sediment or altered basement, was an important process during crustal growth events within the Greenland Shield from ca. 4000 Ma, and became an even more significant process during the Proterozoic.

Detrital zircons of the Mørænesø Formation show a progressive increase in $\delta^{18}O$ from the end of the Archean to the present day, similar to that seen in the global compilation of Valley et al. (2005). In contrast to this earlier study, however, our data set suggests a progressive increase in $\delta^{18}O$ values also during the Archean. These secular changes in $\delta^{18}O$ imply increasing incorporation of high $\delta^{18}O$ material into silicic magmas over time via increased weathering, transport, and reworking of high $\delta^{18}O$ sources. This observation supports models for increasing continental crustal volume during the Archean and the progressive stiffening and exposure of continental crust.

The Mørænesø Formation data set further documents a minor change in the rate of increase of heavy oxygen signatures across the Archean-Proterozoic boundary. This rate change may reflect (1) changing sediment composition from material derived from chemically weathered, buffered solutions in the Archean to mechanically broken-down material in the Proterozoic; and/or (2) a greater abundance of sediment available for recycling due to erosion of longer and higher Proterozoic orogens.

One Eoarchean (3953 ± 18 Ma) grain yields a heavy oxygen isotope signature of 7.8 ± 0.5‰, which is interpreted as a primary magmatic value. This is consistent with the existence of liquid water during Eoarchean times and implies wet melting conditions.

ACKNOWLEDGMENTS

Kirkland wishes to thank J. Ineson, P. Frykman, J.S. Peel, and L. Stemmerik for insightful discussion in the field. Financial support from the Swedish Research Council (to Pease) and Ymer-80 (to Kirkland) is gratefully acknowledged. We thank reviewers Tony Kemp, Anna Pietranik, and Jon Patchett for constructive comments that improved this manuscript. Kirkland and Van Kranendonk publish with the permission of the Executive Director of the Geological Survey of Western Australia. The NORDSIM facility is funded by the research councils of Denmark, Norway, Sweden, the Geological Survey of Finland, and the Swedish Museum of Natural History. This is NORDSIM publication 249.

REFERENCES CITED

Albarède, F., 1998, The growth of continental crust: Tectonophysics, v. 296, no. 1–2, p. 1–14, doi: 10.1016/S0040-1951(98)00133-4.

Allègre, C.J., 1982, Chemical geodynamics: Tectonophysics, v. 81, no. 3–4, p. 109, doi: 10.1016/0040-1951(82)90125-1.

Allègre, C.J., and Rousseau, D., 1984, The growth of continents through geological time studied by Nd isotope analysis of shales: Earth and Planetary Science Letters, v. 67, p. 19–34, doi: 10.1016/0012-821X(84)90035-9.

Allen, P.A., and Leather, J., 2006, Post-Marinoan marine siliciclastic sedimentation: The Masirah Bay Formation, Neoproterozoic Huqf Supergroup of Oman: Precambrian Research, v. 144, no. 3–4, p. 167–198, doi: 10.1016/j.precamres.2005.10.006.

Amelin, Y., Lee, D.-C., Halliday, A.N., and Pidgeon, R.T., 1999, Nature of the Earth's earliest crust from hafnium isotopes in single detrital zircons: Nature, v. 399, p. 252–255, doi: 10.1038/20426.

Cagnard, F., Durrieu, N., Gapais, D., Brun, J.-P., and Ehlers, C., 2006, Crustal thickening and lateral flow during compression of hot lithospheres, with particular reference to Precambrian times: Terra Nova, v. 18, no. 1, p. 72–78, doi: 10.1111/j.1365-3121.2005.00665.x.

Campbell, I., and Allen, C., 2008, Formation of supercontinents linked to increases in atmospheric oxygen: Nature Geoscience, v. 1, p. 554–558, doi: 10.1038/ngeo259.

Cavosie, A.J., Valley, J.W., Wilde, S.A. and Edinburgh Ion Microprobe Facility, 2005, Magmatic $\delta^{18}O$ in 4400–3900 Ma detrital zircons: A record of the alteration and recycling of crust in the Early Archean: Earth and Planetary Science Letters, v. 235, no. 3–4, p. 663–681, doi: 10.1016/j.epsl.2005.04.028.

Cavosie, A.J., Kita, N.T., and Valley, J.W., 2009, Primitive oxygen-isotope ratio recorded in magmatic zircon from the Mid-Atlantic Ridge: The American Mineralogist, v. 94, p. 926–934, doi: 10.2138/am.2009.2982.

Chauvel, C., Lewin, E., Carpentier, M., Arndt, N.T., and Marini, J.-C., 2008, Role of recycled oceanic sediments in generating the hafnium-neodymium mantle array: Nature Geoscience, v. 1, p. 64–67, doi: 10.1038/ngeo.2007.51.

Choukroune, P., Bouhallier, H., and Arndt, N., 1995, Soft lithosphere during periods of Archean crustal growth or crustal reworking, *in* Coward, M., and Ries, A.C., eds., Early Precambrian Processes: Geological Society, London, Special Publication 95, p. 67–86, doi: 10.1144/GSL.SP.1995.095.01.05.

Collerson, K.D., and Kamber, B.S., 1999, Evolution of the continents and the atmosphere inferred from Th-U-Nb systematics of the depleted mantle: Science, v. 283, p. 1519–1522, doi: 10.1126/science.283.5407.1519.

Collinson, J.D., Bevins, R.E., and Clemmensen, L.B., 1989, Post-glacial mass flow and associated deposits preserved in palaeovalleys: The Late Precambrian Mørænesø Formation, North Greenland: Meddelelser om Grønland, v. 269, 27 p.

Condie, K.C., 1993, Chemical composition and evolution of the upper continental crust: Contrasting results from surface samples and shales: Chemical Geology, v. 104, p. 1–37, doi: 10.1016/0009-2541(93)90140-E.

Condie, K.C., 1998, Episodic continental growth and supercontinents: A mantle avalanche connection?: Earth and Planetary Science Letters, v. 163, no. 1–4, p. 97, doi: 10.1016/S0012-821X(98)00178-2.

Condie, K.C., 2004, Supercontinents and superplume events: Distinguishing signals in the geologic record: Physics of the Earth and Planetary Interiors, v. 146, no. 1–2, p. 319, doi: 10.1016/j.pepi.2003.04.002.

Coogan, L.A., and Hinton, R.W., 2006, Do the trace element compositions of detrital zircons require Hadean continental crust?: Geology, v. 34, p. 633–636, doi: 10.1130/G22737.1.

Davies, G.F., 1980, Thermal histories of convective Earth models and constraints on radiogenic heat production in the Earth: Journal of Geophysical Research, v. 85, p. 2517–2530, doi: 10.1029/JB085iB05p02517.

Dawes, P.R., 2006, Explanatory Notes to the Geological Map of Greenland, Thule, Sheet 5: Geological Survey of Denmark and Greenland Map Series 2, scale 1:500,000, 97 p.

Dewing, K., Harrison, J.C., Pratt, H.B., and Mayr, U., 2004, A probable late Neoproterozoic age for the Kennedy Channel and Ella Bay Formations, northeastern Ellesmere Island and its implications for passive margin history of the Canadian Arctic: Canadian Journal of Earth Sciences, v. 41, no. 9, p. 1013–1025, doi: 10.1139/e04-044.

Dickinson, W.R., and Kröner, A., 1981, Plate Tectonics through Geological Time: The Origin and Evolution of the Earth's Continental Crust: Philosophical Transactions of the Royal Society of London, ser. A, Mathematical and Physical Sciences, v. 301, no. 1461, p. 207–215.

Escher, J.C., and Pulvertaft, T.C.R., 1995, Geological Map of Greenland: Copenhagen, Geological Survey of Greenland, scale 1:2,500,000.

Fedo, C.M., Sircombe, K.N., and Rainbird, R.H., 2003, Detrital zircon analysis of the sedimentary record: Reviews in Mineralogy and Geochemistry, v. 53, no. 1, p. 277–303, doi: 10.2113/0530277.

Foulger, G.R., Natland, J.H., Presnall, D.C., and Anderson, D.L., eds., 2005, Plates, Plumes and Paradigms: Geological Society of America Special Paper 388, 997 p.

Franck, S., 1998, Evolution of the global mean heat flow over 4.6 Gyr: Tectonophysics, v. 291, no. 1–4, p. 9–18, doi: 10.1016/S0040-1951(98)00027-4.

Fyfe, W.S., 1978, Evolution of the Earth's crust: Modern plate tectonics to ancient hot spot tectonics?: Chemical Geology, v. 23, p. 89, doi: 10.1016/0009-2541(78)90068-2.

Harrison, T.M., Blichert-Toft, J., Müller, W., Albarède, F., Holden, P., and Mojzsis, S.J., 2005, Heterogeneous Hadean hafnium: Evidence of continental crust at 4.4 to 4.5 Ga: Science, v. 310, p. 1947–1950, doi: 10.1126/science.1117926.

Hawkesworth, C.J., and Kemp, A.I.S., 2006, The differentiation and rates of generation of the continental crust: Chemical Geology, v. 226, p. 134–143, doi: 10.1016/j.chemgeo.2005.09.017.

Henriksen, N., Higgins, A.K., Kalsbeek, F., and Pulvertaft, T.C.R., 2000, Greenland from Archean to Quaternary. Descriptive Text to the Geological Map of Greenland: Geology of Greenland Survey Bulletin 185, scale 1:2,500,000, 93 p. + map.

Hopkins, M., Harrison, T.M., and Manning, C.E., 2008, Low heat flow inferred from >4 Gyr zircons suggests Hadean plate boundary interactions: Nature, v. 456, no. 7221, p. 493, doi: 10.1038/nature07465.

Hurley, P.M., and Rand, J.R., 1969, Pre-drift continental nuclei: Science, v. 164, p. 1229–1242, doi: 10.1126/science.164.3885.1229.

Jean-Baptiste, P., Charlou, J.L., and Stievenard, M., 1997, Oxygen isotope study of mid-ocean ridge hydrothermal fluids: Implication for the oxygen-18 budget of the oceans: Geochimica et Cosmochimica Acta, v. 61, no. 13, p. 2669–2677, doi: 10.1016/S0016-7037(97)00090-2.

Kemp, A.I.S., Hawkesworth, C.J., Paterson, B.A., and Kinny, P.D., 2006, Episodic growth of the Gondwana supercontinent from hafnium and oxygen isotopes in zircon: Nature, v. 439, p. 580–583, doi: 10.1038/nature04505.

King, E.M., Valley, J.W., Davis, D.W., and Edwards, G.R., 1998, Oxygen isotope ratios of Archean plutonic zircons from granite-greenstone belts of the Superior Province: Indicator of magmatic source: Precambrian Research, v. 92, p. 365–387, doi: 10.1016/S0301-9268(98)00082-5.

Kirkland, C.L., Pease, V., Whitehouse, M.J., and Ineson, J.R., 2009, Provenance record from Mesoproterozoic-Cambrian sediments of Peary Land, North Greenland: Implications for the ice-covered Greenland Shield and Laurentian palaeogeography: Precambrian Research, v. 170, p. 43–60, doi: 10.1016/j.precamres.2008.11.006.

Knudsen, T.L., Andersen, T., Whitehouse, M.J., and Vestin, J., 1997, Detrital zircon ages from southern Norway—Implications for the Proterozoic evolution of the southwestern Baltic Shield: Contributions to Mineralogy and Petrology, v. 130, p. 47–58, doi: 10.1007/s004100050348.

Kump, L.R., 2008, The rise of atmospheric oxygen: Nature, v. 451, no. 7176, p. 277–278, doi: 10.1038/nature06587.

Lackey, J.S., Valley, J.W., and Saleeby, J.B., 2005, Supracrustal input into magmas in the deep crust of the Sierra Nevada Batholith: Evidence from high $\delta^{18}O$ zircon: Earth and Planetary Science Letters, v. 235, p. 315–330, doi: 10.1016/j.epsl.2005.04.003.

Lowe, D.R., and Tice, M.M., 2004, Geologic evidence for Archean atmospheric and climatic evolution: Fluctuating levels of CO_2, CH_4, and O_2 with an overriding tectonic control: Geology, v. 32, p. 493–496, doi: 10.1130/G20342.1.

McCulloch, M.T., and Bennett, V.C., 1994, Progressive growth of the Earth's continental-crust and depleted mantle—Geochemical constraints: Geochimica et Cosmochimica Acta, v. 58, p. 4717–4738, doi: 10.1016/0016-7037(94)90203-8.

McLennan, S.M., and Taylor, S.R., 1983, Continental freeboard, sedimentation rates and growth of continental crust: Nature, v. 306, no. 5939, p. 169–172, doi: 10.1038/306169a0.

Moorbath, S., 1985, Crustal evolution in the early Precambrian: Origins of Life and Evolution of the Biosphere, v. 15, no. 4, p. 251–261, doi: 10.1007/BF01808172.

Murakami, T., Chakoumakos, B.C., Ewing, R.C., Lumpkin, G.R., and Weber, W.J., 1991, Alpha-decay event damage in zircon: The American Mineralogist, v. 76, no. 9–10, p. 1510–1532.

Nägler, T.F., and Kramers, J.D., 1998, Nd isotopic evolution of the upper mantle during the Precambrian: Models, data and the uncertainty of both: Precambrian Research, v. 91, p. 233–252, doi: 10.1016/S0301-9268(98)00051-5.

Nemchin, A.A., Pidgeon, R.T., and Whitehouse, M.J., 2006a, Re-evaluation of the origin and evolution of > 4.2 Ga zircons from the Jack Hills metasedimentary rocks: Earth and Planetary Science Letters, v. 244, no. 1–2, p. 218–233, doi: 10.1016/j.epsl.2006.01.054.

Nemchin, A.A., Whitehouse, M.J., Pidgeon, R.T., and Meyer, C., 2006b, Oxygen isotopic signature of 4.4–3.9 Ga zircons as a monitor of differentiation processes on the Moon: Geochimica et Cosmochimica Acta, v. 70, no. 7, p. 1864–1872, doi: 10.1016/j.gca.2005.12.009.

Nutman, A.P., Dawes, P.R., Kalsbeek, F., and Hamilton, M.A., 2008, Palaeoproterozoic and Archean gneiss complexes in northern Greenland: Palaeoproterozoic terrane assembly in the high Arctic: Precambrian Research, v. 161, p. 419–451, doi: 10.1016/j.precamres.2007.09.006.

O'Neil, J.R., and Chappell, B.W., 1977, Oxygen and hydrogen isotope relations in the Berridale Batholith: Journal of the Geological Society, v. 133, p. 559–571, doi: 10.1144/gsjgs.133.6.0559.

O'Nions, R.K., Evenson, N.M., Hamilton, P.J., and Carter, S.R., 1978, Melting of the mantle past and present: Isotope and trace element evidence: Philosophical Transactions of the Royal Society of London, ser. A, Mathematical and Physical Sciences, v. 258, p. 547–559.

Peck, W.H., King, E.M., and Valley, J.W., 2000, Oxygen isotope perspective on Precambrian crustal growth and maturation: Geology, v. 28, p. 363–366, doi: 10.1130/0091-7613(2000)28<363:OIPOPC>2.0.CO;2.

Peck, W.H., Valley, J.W., Wilde, S.A., and Graham, C.M., 2001, Oxygen isotope ratios and rare earth elements in 3.3 to 4.4 Ga zircons: Ion microprobe evidence for high $\delta^{18}O$ continental crust and oceans in the Early Archean: Geochimica et Cosmochimica Acta, v. 65, no. 22, p. 4215–4229, doi: 10.1016/S0016-7037(01)00711-6.

Peck, W.H., Valley, J.W., and Graham, C.M., 2003, Slow oxygen diffusion rates in igneous zircons from metamorphic rocks: The American Mineralogist, v. 88, no. 7, p. 1003–1014.

Rainbird, R.H., Hearnan, L.M., and Young, G., 1992, Sampling Laurentia: Detrital zircon geochronology offers evidence for an extensive Neoproterozoic river system originating from the Grenville orogen: Geology, v. 20, p. 351–354, doi: 10.1130/0091-7613(1992)020<0351:SLDZGO>2.3.CO;2.

Rey, P., and Houseman, G., 2006, Lithospheric gravitational flow: The impact of body forces on orogenic processes from Archean to Phanerozoic, *in* Buiter, S.J.H., and Schreurs, G., eds., Analogue and Numerical Modelling of Crustal-Scale Processes: Geological Society, London, Special Publication 253, p. 153–167, doi: 10.1144/GSL.SP.2006.253.01.08.

Rollinson, H., 2008, Ophiolitic trondhjemites: A possible analogue for Hadean felsic 'crust': Terra Nova, v. 20, p. 364–369, doi: 10.1111/j.1365-3121.2008.00829.x.

Rudnick, R., and Fountain, D., 1995, Nature and composition of the continental crust: A lower crustal perspective: Reviews of Geophysics, v. 33, p. 267–309, doi: 10.1029/95RG01302.

Scholl, D.W., and von Huene, R., 2009, Implications of estimated magmatic additions and recycling losses at the subduction zones of accretionary (non-collisional) and collisional (suturing) orogens, *in* Cawood, P., and Kröner, A., eds., Earth Accretionary Systems in Space and Time: Geological Society, London, Special Publication 318, p. 105–125, doi: 10.1144/SP318.4.

Shirey, S.B., Kamber, B.S., Whitehouse, M.J., Mueller, P.A., and Basu, A.R., 2008, A review of the isotopic and trace element evidence for mantle and crustal processes in the Hadean and Archean: Implications for the onset of plate tectonic subduction, *in* Condie, K.C., and Pease, V., eds., When Did Plate Tectonics Begin on Planet Earth?: Geological Society of America Special Paper 440, p. 1–29, doi: 10.1130/2008.2440(01).

Squire, R., Campbell, I., Allen, C., and Wilson, C., 2006, Did the Transgondwanan Supermountain trigger the explosive radiation of animals on Earth?: Earth and Planetary Science Letters, v. 250, p. 116–133, doi: 10.1016/j.epsl.2006.07.032.

Surlyk, F., 1991, Tectonostratigraphy of North Greenland, *in* Peel, S.J., and Sonderholm, M., eds., Sedimentary Basins of North Greenland: Grønlands Geologiske Undersøgelse, p. 25–47.

Taylor, S.R., and McLennan, S.M., 1981, The composition and evolution of the continental crust: Rare earth element evidence from sedimentary rocks: Philosophical Transactions of the Royal Society of London, ser. A, Mathematical and Physical Sciences, v. 301, p. 381–399, doi: 10.1098/rsta.1981.0119.

Upton, B.G.J., Rämå, O.T., Heaman, L.M., Blichert-Toft, J., Kalsbeek, F., Barry, T.L., and Jepsen, H.F., 2005, The Mesoproterozoic Zig-Zag Dal basalts and associated intrusions of eastern North Greenland: Mantle plume–lithosphere interaction: Contributions to Mineralogy and Petrology, v. 149, p. 40–56, doi: 10.1007/s00410-004-0634-7.

Valley, J.W., 2003, Oxygen isotopes in zircon: Reviews in Mineralogy and Geochemistry, v. 53, no. 1, p. 343–385, doi: 10.2113/0530343.

Valley, J., Peck, W., King, E., and Wilde, S., 2002, A cool early Earth: Geology, v. 30, p. 351–354, doi: 10.1130/0091-7613(2002)030<0351:ACEE>2.0.CO;2.

Valley, J.W., Lackey, J.S., Cavosie, A.J., Clechenko, C.C., Spicuzza, M.J., Basei, M.A.S., Bindeman, I.N., Ferreira, V.P., Sial, A.N., King, E.M., Peck, W.H., Sinha, A.K., and Wei, C.S., 2005, 4.4 billion years of crustal maturation; oxygen isotope ratios of magmatic zircon: Contributions to Mineralogy and Petrology, v. 150, p. 561–580, doi: 10.1007/s00410-005-0025-8.

Veizer, J., and Compston, W., 1976, $^{87}Sr/^{86}Sr$ in Precambrian carbonates as an index of crustal evolution: Geochimica et Cosmochimica Acta, v. 40, p. 905–914, doi: 10.1016/0016-7037(76)90139-3.

Wanke, H., Dreibus, G., and Jagoutz, E., 1984, Mantle geochemistry and accretion history of the Earth, *in* Kröner, A., Hanson, G.N., and Goodwin, A.M., eds., Archean Geochemistry: Berlin, Springer-Verlag, p. 1–24.

Whitehouse, M.J., and Nemchin, A.A., 2009, High precision, high accuracy measurement of oxygen isotopes in a large lunar zircon by SIMS: Chemical Geology, v. 261, p. 32–42, doi: 10.1016/j.chemgeo.2008.09.009.

Wiedenbeck, M., Hanchar, J.M., Peck, W.H., Sylvester, P., Valley, J., Whitehouse, M., Kronz, A., Morishita, Y., Nasdala, L., Fiebig, J., Franchi, I., Girard, J.-P., Greenwood, R.C., Hinton, R., Kita, N., Mason, P.R.D., Norman, M., Ogasawara, M., Piccoli, P.M., Rhede, D., Satoh, H., Schulz-Dobrick, B., Skår, O., Spicuzza, M., Terada, K., Tindle, A., Togashi, S., Vennemann, T., Xie, Q., and Zheng, Y.-F., 2004, Further characterisation of the 91500 zircon crystal: Geostandards and Geoanalytical Research, v. 28, no. 1, p. 9–39, doi: 10.1111/j.1751-908X.2004.tb01041.x.

Wilde, S.A., Valley, J.W., Peck, W.H., and Graham, C.M., 2001, Evidence from detrital zircons for the existence of continental crust and oceans on the Earth 4.4 Gyr ago: Nature, v. 409, no. 6817, p. 175, doi: 10.1038/35051550.

MANUSCRIPT RECEIVED 15 SEPTEMBER 2009
REVISED MANUSCRIPT RECEIVED 20 DECEMBER 2009
MANUSCRIPT ACCEPTED 21 DECEMBER 2009

Printed in the USA